Reverse analysis in depth-sensing indentation for thin films Young's modulus evaluation

Jorge Manuel Antunes, José Valdemar Fernandes, Nataliya Sakharova, Luís Menezes

Reverse analysis in depth-sensing indentation for thin films Young's modulus evaluation

Journal:	*Philosophical Magazine & Philosophical Magazine Letters*
Manuscript ID:	TPHM-07-Feb-0062.R1
Journal Selection:	Philosophical Magazine
Date Submitted by the Author:	27-Nov-2007
Complete List of Authors:	Antunes, Jorge; Instituto Politécnico de Tomar Fernandes, José; Universidade de Coimbra Sakharova, Nataliya; Universidade de Coimbra Menezes, Luís; Universidade de Coimbra
Keywords:	nanoindentation, thin films
Keywords (user supplied):	Reverse analysis, numerical simulation

Reverse analysis in depth-sensing indentation for thin films

Young's modulus evaluation

J.M. ANTUNES [*,a], J.V. FERNANDES [b], N.A. SAKHAROVA [b], L.F. MENEZES [b]

[a] *Escola Superior de Tecnologia de Abrantes, Instituto Politécnico de Tomar,*

Rua 17 de Agosto de 1808, 2200 Abrantes, Portugal.

[b] *CEMUC – Departamento de Engenharia Mecânica – Faculdade de Ciências e Tecnologia,*

Polo 2 da Universidade de Coimbra – Pinhal de Marrocos, P-3030-201 Coimbra, Portugal.

[*] Corresponding author. Tel.: + (351) 239 790700; fax.: + (351) 239 790701.
E-mail address: jorge.antunes@dem.uc.pt

Abstract

This paper seeks to present an approach to reverse analysis in depth-sensing indentation of composite film/substrate materials, which makes use of numerical simulation. This methodology allows the results of experimental hardness tests, acquired with pyramidal indenter geometry, to be used to determine the Young's modulus of thin film materials. Forward and reverse analyses were performing making use of three-dimensional numerical simulations of pyramidal and flat punch indentation tests in order to determine the Young's modulus of the thin films. The pyramidal indenter used in the numerical simulations takes into account the presence of the most common imperfection of the tip, so-called offset. The contact friction between the Vickers indenter and the deformable body is also considered. The forward analysis uses fictitious composite materials with different relationships between the values of the Young's modulus of the film and substrate. The proposed reverse analysis procedure provides a unique value for the film's Young's modulus. Depending on the material properties, the value of the Young's modulus of the film can be more or less sensitive to the scatter of the experimental results, obtained using the depth-sensing equipment. The validity of the proposed reverse analysis method is checked using four real cases of composite materials.

Keywords: Reverse analysis, thin films, numerical simulation

1. Introduction

In the mechanical characterization of composite film/substrate materials, one of the most important properties is the Young's modulus of the film. For this purpose depth-sensing indentation with spherical or pyramidal indenters is the usual method. However, the determination of the Young's modulus of the film requires low indentation depths, which is challenging in the case of very thin films, because the composite elastic response deviates from that of the film, for indentation depths above around 1-2% of the thickness (e.g. [1]). The usual solution for this problem consists of performing higher indentation depths in tests, and then separating the contribution of the film from the composite Young's modulus results. The mechanical properties of the composite are a complex function of the film and substrate's mechanical properties, which depend on the maximum applied load [2-7]. In this context, the knowledge of the film and substrate's effects on the evaluated mechanical properties of the composite is important. In several previous experimental and theoretical studies, different methods were proposed for extracting the Young's modulus of thin films. In general, Young's modulus of the film is determined using phenomenological and empirical analytical models (e.g. [8-11]).

Recently, reverse analysis methods have been proposed for determining the elastic and plastic properties of bulk materials (e.g. [12-14]). To our knowledge, no such procedures have been developed for thin films, namely for the determination of Young's modulus. The main objective of this study is to present a three-dimensional numerical simulation method for predicting the Young's modulus of the film from the results of depth sensing indentation experiments on composite film/substrate materials. To this purpose, forward analysis was applied to the results of the three-dimensional numerical simulations of Vickers hardness tests and flat punch tests of several composite materials, which allows equivalence between the results of both types of tests to be established. Reverse analysis was proposed based on this conclusion, which consists of a simple methodology for predicting the film's Young's modulus. The accuracy and sensitivity to the ratio of the film and substrate's Young's modulus of the proposed reverse analysis method were also examined, in the particular cases of four composite materials.

2. Methodology review of depth sensing indentation of films

Using depth-sensing indentation, the Young's modulus of the sample is determined from:

$$E^{SI} = \frac{1}{\beta}\frac{\sqrt{\pi}}{2}\frac{1}{\sqrt{A}}\frac{1}{C}, \quad (1)$$

where β is a correction factor depending on the indenter geometry. A is the contact area of the indentation and C is the compliance. E^{SI} is the "specimen + indenter" modulus. The specimen Young's modulus E, that depends on the film and substrate's elastic modulus (E_f and E_s, respectively), is evaluated using the definition:

$$\frac{1}{E^{SI}} = \frac{1}{E^*} + \frac{1}{E_i^*}, \quad (2)$$

with

$$E^* = E/(1-\nu^2) \text{ and } E_i^* = E_i/(1-\nu_i^2), \quad (3)$$

where, E^* and E_i^* are the reduced modulus and ν and ν_i are the Poisson's ratios of the specimen and of the indenter, respectively. In the case of elastically homogeneous composites, film and substrate have the same reduced Young's modulus and so $E^* = E_f^* = E_s^*$. If the film and substrate are not elastically homogeneous, the reduced modulus evaluated with Eq. (1) does not correspond only to the film, especially if the film is very thin and/or the ratio between the Young's modulus of the film and substrate is very different from 1. When the reduced Young's modulus of the film, E_f^*, and the substrate, E_f^*, differs, the evaluated reduced indentation modulus of the specimen, E^*, depends on the indentation depth. By increasing the indentation depth, the specimen's reduced Young's modulus changes gradually from the value of the film to the one of the substrate. In fact, the composite elastic response deviates from that of the film above a ratio indentation depth to film thickness around 1-2% [1].

For the case where higher maximum indentation depths are used weight functions, which take into account the contributions of the film and the substrate, have been proposed as a means of evaluating the film's Young's modulus. The determination of the film's Young's modulus consists of fitting these weight functions to the experimental composite elastic modulus results *versus* the contact indentation depth, h,

normalized by the film thickness, t, and extrapolating the measured Young's modulus values to zero penetration (e.g. [10, 15]). These types of methodologies present difficulties (e.g. [10]), namely the accuracy of the film's Young's modulus evaluation depends on the number and the range of the values of the maximum load (or indentation depth), experimentally used for composite Young's modulus determination, when using a specified model. The minimum value of the experimental maximum penetration depth is usually limited by the error of the measured E^* value, which increases when the maximum penetration depth increases, while the maximum value of the experimental maximum penetration depth is sometimes limited by film cracking or delamination. Furthermore, the performance of the models is strongly influenced by the ratio between the film and substrate Young's modulus.

2. Numerical simulation

2.1. *Finite element code*

In the numerical simulations of the hardness tests, the HAFILM code was used. This code was specifically developed to simulate hardness tests with any type of indenter shape taking into account contact with friction between the indenter and the sample [16]. The mechanical model that is the basis of the HAFILM code considers the hardness test as a quasi-static process that occurs in the domain of large deformation problems. One of the most common difficulties with the numerical simulation of the indentation process is related to the time dependence of the boundary conditions due to the contact with friction between the indenter, assumed to be rigid, and the deformable body. In HAFILM, the contact with friction problem is modelled using a classical Coulomb law. To associate the static equilibrium problem with the contact with friction, an augmented Lagrangean method is applied to the mechanical formulation. This leads to a system of non linear equations, where the kinematic (material displacements) and static variables (contact forces) are the final unknowns of the problem [17]. In order to solve it, the code makes use of a fully implicit Newton-Raphson type algorithm. All non-linearities, induced by the elastoplastic behaviour of the material and by the contact with friction, are treated in a single iterative loop [17]. The friction between the indenter and the deformable body was assumed to have a friction coefficient of 0.16. This is a commonly used value and leads to a better description of the indentation process than if frictionless contact were assumed [16, 18].

2.2. *Finite element mesh and indenters*

The sample used in the numerical simulation was discretised into isoparametric solid finite elements associated with a selective reduced integration method that enables the elements' performance to improve when large plastic deformations are assumed. Due to geometrical symmetry in the X=0 and Z=0 planes, only a fourth of the sample was used in the numerical simulations. The finite element mesh was composed of 9072 three-linear eight-node isoparametric hexahedrons [18]. The film thickness of the sample was 0.5 μm . Previous studies of the sensitivity of the mesh have improved its performance significantly, guaranteeing reliable estimation of the indentation contact area [18].

In the simulations, it was assumed that the Vickers indenter had an indenter tip imperfection: a rectangular planed area (with one side twice the length of the other) with an area of 0.0288 μm^2 was used instead of the ideal tip [16, 19]. This indenter tip imperfection is similar that of the experimental Vickers indenter tip. In addition, several flat punch indenters with square geometry and different contact areas were used in the numerical simulations. Table 1 presents the seven flat punch indenters used in the numerical simulations. The geometries of both types of indenter, Vickers and flat punches, were modulated using Bézier surfaces.

[Insert table 1 about here]

3. Direct analysis

This analysis starts by the comparison of the composite Young's modulus results determined by the numerical simulation, using the pyramidal Vickers and flat punch indenters. The numerical simulations involve seven fictitious composites modulated by different values of the ratio between the film and substrate Young's modulus (E_f/E_s). The Poisson ration, ν, was 0.30 both for film and substrate . To simplify, the composites' plastic mechanical properties are such that the ratio between the film and substrate yield stress, σ_f/σ_s, is 1 (three composites with a σ_f/σ_s ratio of 2 confirmed the results obtained for the $\sigma_f/\sigma_s = 1$ composites). The plastic behaviour of the fictitious materials of the composites were modulated by the Swift law: $\sigma = k(\varepsilon + \varepsilon_0)^n$, where σ and ε are the von Mises equivalent stress and plastic strain, respectively, and k, ε_0 and n are material constants (the material yield stress is: $\sigma_y = k\varepsilon_0^n$). The film and substrate materials were considered without work-hardening (n, was close to zero).

Table 2 summarizes the mechanical properties of the composites used in the numerical simulations.

[Insert table 2 about here]

In the case of the tests with the Vickers indenter the composite elastic modulus was determined using Eq. (1), where the correction factor, β, was considered as 1.05 [18]. The contact area, A, was evaluated by the contour of the nodes in the finite element mesh in contact with the indenter at the maximum load. The compliance C was evaluated from the unloading curve using the typical procedure (e.g. [18]). In the case of the hardness tests with the flat punch indenters, the Young's modulus was evaluated using Sneddon's relation [20]:

$$F = \frac{2E}{(1-\nu^2)} a h_e, \quad (4)$$

where F is the applied load, E the Young's modulus, ν the Poisson ratio, a the radius of the flat punch indenter and h_e the elastic indentation depth. In order that the attributes of pyramidal and flat punch indenters are as similar as possible, we use flat punch indenters with square geometry, where a (in Eq. (4)) corresponds to the radius of circular indenter with the same area than the squared one. As Eq. (4) was deduced for circular flat punch indenters, preliminary numerical simulations on different bulk materials were performed, in order to investigate the requirement of using a β factor (with the same meaning as in Eq. (1)), when using Eq. (4) for the case of square flat punch indenters. It was concluded that, even for this geometry, this equation describes the elastic behaviour of the samples well, without needing a β factor different from 1 (in Eq. (4)): the output values of simulations were similar to the input values, having errors lower than $\pm 1\%$.

When using a flat punch indenter, only elastic deformation is attained in the sample for low indentations depths. The load, F, versus the elastic indentation depth, h_e, relationship follows a linear fit, allowing the value $2E^* a$ to be determined, where $E^* = E/(1-\nu^2)$ is the reduced elastic modulus of the composite and $a = \sqrt{(A/\pi)}$ is the equivalent indentation contact radius, corresponding to the area A of the square indentation punch. Figure 1 shows two examples of these linear evolutions, obtained by numerical simulation of the composites C1 and C7 (E_f/E_s equal to 4 and 0.25, respectively) with seven different areas of flat indenters.

[Insert figure 1 about here]

Figure 2 shows the comparison of the evolution of the composite elastic modulus, E, as a function of the normalized indentation depth, h/t (composites C1, C2, C3, C4, C5, C6 and C7), obtained by the numerical simulation with the Vickers and squared flat punch indenters. For the case of the flat punch indenter, an equivalent contact indentation depth was defined corresponding to the contact indentation depth of the ideal pyramidal indenter with the same contact area: $h = \sqrt{24.5A}$. Figure 2 shows that the results of the Young's modulus' evolution as a function of the normalized indentation depth do not depend on the type of indenter (pyramidal or flat punch). In the case of composite C5 where $E_f/E_s = 1$ (figure 2 (a)), similar results of the Young's modulus were obtained with the two different indenter geometries, which are very analogous to the input values (E = 200 GPa). Results of figure 2 (a) also demonstrate that is appropriate to use correction factor $\beta = 1$ for the case of the squared flat punches. Also, the composites with the E_f/E_s ratio different from 1 (figure 2 (b) and (c), respectively) show unreservedly a similar evolution of E *versus* h/t, for both indenter geometries.

[Insert figure 2 about here]

4. Reverse analysis

In the context of the above results and considerations, a reverse analysis methodology to determine the Young's modulus of films was developed, based on the similarity of the Young's modulus results determined for the composite using experimental hardness tests with pyramidal indenters (Vickers, but also Berkovich geometry can be used) to the numerical simulation results with flat punch indenters, obtained for the same equivalent indentation contact depth. To this end, an experimental indentation test must be performed up to a specific value of the contact indentation depth, in order to determine the corresponding Young's modulus of the composite. Afterwards, the numerical simulation of the flat punch indenter hardness tests is performed in such away that the ratio between the equivalent contact penetration depth and the film thickness, h/t, is equal to that of the experimental pyramidal test (i.e., the contact area is the same for both tests, experimental and numerical). Since only elastic deformation occurs during the first stages of the flat punch test, knowledge of the plastic mechanical properties of the film and the substrate are not need for the simulation. If the

finite element code uses these properties as input data, those of the substrate material can be used for the substrate and for the film; otherwise, arbitrary values can be chosen. When using the substrate and film's Young's modulus as input data in the code, the first must be previously known (determined by depth sensing indentation, for example) and for the second an arbitrary value must be chosen. This arbitrary value for the film Young's modulus, $E_f^{i=1}$, must be higher than the one experimentally determined for the composite, E, if $E > E_s$ and lower if $E < E_s$.

The value of the Young's modulus of the composite evaluated by numerical simulation using the flat punch indenter, $E^{i=1}$ (when $E_f^{i=1}$, is used to modulate the film), is then compared with the one experimentally determined with the pyramidal indenter E. If the two values of the Young's modulus ($E^{i=1}$ and E) are equal or similar (within a predefined range of accuracy), then the Young's modulus of the film experimentally tested is $E_f = E_f^{i=1}$. If there is too great a difference between the experimental (pyramidal) and numerical (flat punch) composite Young's modulus (this is generally the case), then an iterative method will be used for optimization: if $E^{i=1} > E$, a new arbitrary value for the film Young's modulus $E_f^{i=2}$ must be chosen higher than $E_f^{i=1}$; if $E^{i=1} < E$, a new arbitrary value of $E_f^{i=2}$ must be lower than $E_f^{i=1}$. The iterative process ends when the two values of the composite Young's modulus, numerical and experimental (E^i and E) are equal or similar (within a predefined range of accuracy); the Young's modulus of the film experimentally tested is therefore $E_f = E_f^i$. Figure 3 presents the reverse analysis algorithm for determining a film's Young's modulus. As can be seen in the following numerical examples, this iterative method can be simplified, because an almost linear relationship was found between E^i and E_f^i.

[Insert figure 3 about here]

A purely numerical example of reverse analysis for evaluation of the elastic modulus of the films of two fictitious composites was performed. The thicknesses of the films were 0.50 μm (composites C3 and C6 – table 2). For each composite, numerical simulations of the hardness test with a pyramidal Vickers indenter were performed up to two different values of the normalized contact indentation depth (h/t = 0.2 and 1.3 for composite C3 and h/t = 0.3 and 1.3 for composite C6). Table 3 summarizes the values of the contact areas, the normalized contact indentation depths, and the composite

reduced Young's modulus, obtained in these tests. These forward values will be used as "experimental" values in this analysis. Four flat punch square indenters, with areas equal to the indentation contact areas of the pyramidal tests were defined, in order to perform numerical tests with contact indentation depths, h/t, equal to the pyramidal Vickers test. The algorithm of figure 3 was then used to determine the values of the films' Young's moduli, E_f^i, and the correspondent composite Young's moduli E^{i}, using the flat punch indenter. Figure 4 shows an almost linear plot of E^{i} *versus* E_f^i, for the cases analyzed. This allows us to simplify the iterative method: after obtaining two or three results ($E_f^i ; E^{\mathrm{i}}$), corresponding to the open symbols in figure 4, high-quality estimation for E_f^i can be obtained, by using the linear plot of these results. In fact, a good evaluation $\mathrm{E_f^i} \approx \mathrm{E_f}$ corresponds to $E^i = E$ on the linear plot (solid symbols in figure 4). In order to refine the reverse analysis, the algorithm of figure 3 can be used again (if necessary). Table 4 show these values and the associated error, for the four cases of reverse analysis performed. The film Young's modulus results are highly accurate, but they are better for $h/\mathrm{t} = 0.2$ (errors of 0.83 and 1,00 %, for C3 and C9 composites, respectively) than for $h/\mathrm{t} = 1.3$ (errors of 4.17 and 2,00 %, for C3 and C9 composites, respectively). In fact, with increasing indention depth, the values of the composite and substrate Young's modulus become close, and the method becomes less sensitive. But, even for a such high value of $h/\mathrm{t} = 1.3$, the results are highly accurate.

[Insert table 3 about here]

[Insert table 4 about here]

[Insert figure 4 about here]

5. Reverse analysis of real composite materials

In order to further check the validation of the proposed reverse analysis methodology, a study was performed using the results of real composites. The experimental data is obtained from Mencík et al. [10] and Saha and Nix [6]. Table 5 summarizes the elastic constants of the film and substrate materials of these studies. Composites were selected with values of the E_f/E_s ratio lower and higher than one. For each case, two especially different values of this ratio were chosen, in order to investigate composites within a wide range of values of the E_f/E_s ratio: two composites

for which the ratio E_f/E_s is relatively close to 1 (E_f/E_s = 0.75 and 2.01) and the other two composites have the ratio E_f/E_s relatively far from 1 (E_f/E_s = 0.17 and 5.47), as shown in table 5.

[Insert table 5 about here]

From the study of Mencík et al. [10], two composites obtained by the combination of the film TbFe+Fe with two substrates, silicon and glass, were studied. This combination enables composites with $E_f < E_s$ and $E_f > E_s$ (E_f/E_s = 0.75 and 2.01, respectively) to be obtained. Figure 5 (a) shows the evolution of the composite reduced Young's modulus values, E^*, *versus* the relative indentation depth, h/t. The two remaining real composites used in the validation of this reverse analysis methodology were aluminium and tungsten films deposited on sapphire and aluminium substrates (E_f/E_s equal to 0.17 and 5.47 for the composites Aluminium/Sapphire and Tungsten/Aluminium, respectively). Figure 5 (b) shows the evolution of the composite Young's modulus values, E, *versus* the relative indentation depth, h/t. These experimental results were obtained from the study performed by Saha and Nix [6].

[Insert figure 5 about here]

The reverse analysis algorithm for the determination of the films' Young's modulus for these composites, used the experimental results in the range of the relative indentation depths, h/t, between at about 0.2 and 0.3 (see Fig 5). These relative indentation depths are high enough to allow the determination of accurate values of the experimental contact area and consequently of the Young's modulus for the film thickness (table 5), with a moderating influence of the substrate on the composite Young's modulus (figure 5). For higher relative indentation depths the values of composite and substrate Young's modulus become close, and consequently the method is less sensitive. For experimental values of relative indentation depth, h/t, in the above mentioned range, flat punch indenters (square geometry) were used, with a contact area equal to the contact area of the respective pyramidal indentation. Table 6 shows the average values of the films' Young's modulus obtained by the reverse analyses procedure. In general, the results in table 6 agree well with the expected values. The error in the evaluation of the Young's modulus is lower than 6%.

[Insert table 6 about here]

6. Conclusions

A finite element study using the three-dimensional numerical simulation of hardness tests of elastic-plastic composite materials was presented. A reverse analyses methodology was proposed for the determination of the films' Young's moduli. This method is based in the comparison of the composite Young's modulus evaluated in the experimental hardness tests using a pyramidal indenter with that obtained in the numerical simulation with flat punch indenters, for the same values of equivalent relative contact indentation depth h/t. The proposed reverse analysis brings simplicity, swiftness and accuracy to the determination of a film's Young's modulus. It is important to note that no special software is needed to perform the numerical simulations of the hardness tests with flat indenters. A great number of commercial codes can be used to combine the proposed reverse analyses methodology[1].

Finally, this reverse analysis approach consists of an uncomplicated method, which avoids the fitting of analytical models to extensive experimental results of composite Young's modulus, obtained by depth sensing indentation. Moreover, at this point, we believe that this approach to reverse analysis presents new prospects for the entire mechanical characterization of thin films, leading to great improvements in the determination of their plastic behaviour.

Acknowledgements

The authors are grateful to the Portuguese Foundation for Science and Technology (FCT) who financially supported this work, through the Program POCI 2010 (Portuguese Government and FEDER). One of the authors, N.A. Sakharova, was supported by a grant for scientific research from the Portuguese Science and Technology Foundation. This support is gratefully acknowledged.

[1] In addition, the authors are available to perform the simulations using our own home code. Please contact us.

References

[1] F. Cleymand, O. Ferry, R. Kouitat, A. Billard, J. von Stebut, Surf. Coating Technol. **200** 890 (2005).

[2] T.Y. Tsui, J. Vlassak, W.D. Nix, J. Mater. Res. **14** 2196 (1999).

[3] T.Y. Tsui, J. Vlassak, W.D. Nix, J. Mater. Res. **14** 2204 (1999).

[4] B.D. Fabes, W.C. Oliver, R.A. McKee, F.J. Walker, J. Mater. Res.; **7** 3056 (1992).

[5] N.G. Chechenin, J. Bottiger, J.P. Krog, Thin Solid Films; **261** 219 (1995)

[6] R. Saha, W.D. Nix, Acta Mater **50** 23 (2002).

[7] T.F. Page, S.V. Hainsworth, Surf. Coating Technol. **61** 201 (1993).

[8] D.L. Joslin, W.C. Oliver, J. Mater. Res. **5** 123 (1990).

[9] A.M. Korsunsky, M.R. McGurk, S.J. Bull, T.F. Page, Surf. Coating Technol. **99** 171 (1998).

[10] J. Menčík, D. Munz, E. Quandt, E.R. Weppelmann, M.V. Swain, J. Mater. Res. **12** 2475 (1997).

[11] T.Y. Tsui, G.M. Pharr, J. Mater. Res. **14** 292 (1999).

[12] J.M. Antunes, J.V. Fernandes, L.F. Menezes, B.M. chaparro, Acta. Mater. **55** 69 (2007).

[13] S. Swaddiwudhipong, K.K. Tho, Z.S. Lui, K. Zeng, Int. J. Solids Struct. **42** 69 2005.

[14] M. Dao, N. Chollacoop, T.A. Venkatesh, S. Suresh, Acta Mater. **49** 3899 (2001).

[15] J.M. Antunes, J.V. Fernandes, L.F. Menezes, N.A. Sakharova. Surf. Coating Technol, Submited (2007).

[16] J.M. Antunes, L.F. Menezes, J.V. Fernandes, Int. J. Solids Struct, In press.

[17] L.F. Menezes, C. Teodosiu, J. Mater. Process Techon, **97** 100 (2000).

[18] J.M. Antunes, L.F. Menezes, J.V. Fernandes, Int. J. Solids Struct. **43** 784 (2006).

[19] J.M. Antunes, A. Cavaleiro, L.F. Menezes, M.I. Simões, J.V. Fernandes, Surf Coating Technol. **149** 27 (2002).

[20] I.N. Sneddon, Int. J. Engin. Science **3** 47 (1965).

Figure captions

Figure 1. Load *versus* elastic indentation depth, obtained by numerical simulation, using squared flat punch indenters with seven different contact areas: (a) Composite C1 ($E_f / E_s = 4$); (b) Composite C7 ($E_f / E_s = 0.25$).

Figure 2. Composite Young's modulus *versus* normalized contact indentation depth, determined with pyramidal and flat punch indenters: (a) $E_f = E_s$; (b) $E_f < E_s$; (c) $E_f > E_s$.

Figure 3. Reverse analyses algorithm for thin film Young's modulus determination.

Figure 4. Composite Young's modulus ($E = E^i$) *versus* the film Young's modulus ($E_f = E_f^i$), obtained for the composites C3 and C6, at two different equivalent contact indentation depths: (a) Composite C3 and $h/t = 0.2$; (b) Composite C3 and $h/t = 1.3$; (c) Composite C6 and $h/t = 0.3$; (d) Composite C6 and $h/t = 1.3$.

Figure 5. Composite Young's modulus *versus* relative indentation depth. (a) Experimental data by Menčík *et al.* [10]: Composites (TbFe+Fe)/Silicon and (TbFe+Fe)/Glass. (b) Experimental data by Saha and Nix [6]: Composites Tungsten/Aluminium and Aluminium/Sapphire.

Table captions

Table 1. Flat punch indenters with square geometry. The equivalent contact indentation depth, corresponds to the contact depth, h, of the ideal pyramidal indentation, with the same contact area, A: ($h = \sqrt{A/24.5}$)

Table 2. Mechanical properties of the fictitious composites.

Table 3. Normalized indentation depths, contact areas and composite Young's modulus, obtained in the numerical simulation of the Vickers hardness tests.

Table 4. Films Young's modulus, obtained with the algorithm of figure 3.

Table 5. Elastic constants of the real materials. Experimental data by Menčík et al. [10] and Saha and Nix [6].

Table 6. Average values for the films Young's modulus (E_f), obtained by using the algorithm of reverse analyses procedure, shown in figure 3. For comparison, the correspondent values of table 5 ($E_{f(Table\ 5)}$) are also shown.

Tables

Table 1. Flat punch indenters with square geometry. The equivalent contact indentation depth, corresponds to the contact depth, h, of the ideal pyramidal indentation, with the same contact area, A: ($h = \sqrt{A/24.5}$)

Flat indenters	Q1	Q2	Q3	Q4	Q5	Q6	Q7
Contact area (μm^2)	0.25	1.00	2.25	4.00	6.25	9.00	12.25
Equivalent contact indentation depth (μm)	0.101	0.202	0.303	0.404	0.505	0.606	0.707

Table 2. Mechanical properties of the fictitious composites.

Composites	σ_f (GPa)	σ_s (GPa)	n	E_f (GPa)	E_s (GPa)	ε_0	ν	σ_f/σ_s	E_f/E_s
C1				400	100				4
C2				300	100				3
C3				600	200				3
C4	2	2	0.01	400	200	0.005	0.3	1	2
C5				200	200				1
C6				100	200				0.5
C7				100	400				0.25

Table 3. Normalized indentation depths, contact areas and composite Young's modulus, obtained in the numerical simulation of the Vickers hardness tests.

Composites	h/t	A (μm^2)	E (GPa)
C3	0.20	0.52	317.226
	1.30	12.45	234.871
C9	0.30	0.84	134.771
	1.30	12.35	173.628

Table 4. Films Young's modulus, obtained with the algorithm of figure 3.

Composites	h/t	E_f (GPa)	$E_{f(\text{Table 2})}$ (GPa)	Error (%)
C3	0.20	595	600	0.83
	1.30	625	600	4.17
C9	0.30	99	100	1.00
	1.30	102	100	2.00

Table 5. Elastic constants of the real materials. Experimental data by Menčík et al. [10] and Saha and Nix [6].

Composites	Film thickness (μm)	E_f (GPa)	E_s (GPa)	ν_f	ν_s	E_f/E_s
(TbFe+Fe)/Glass [10]	1.20	130.0	64.8	0.30	0.24	2.01
(TbFe+Fe)/Silicon[10]	1.20	130.0	173.8	0.30	0.20	0.75
Aluminium/Sapphire [6]	0.50	70.0	440.0	0.25	0.25	0.17
Tungsten/Aluminium [6]	0.64	400.0	70.0	0.25	0.25	5.47

Table 6. Average values for the films Young's modulus (E_f), obtained by using the algorithm of reverse analyses procedure, shown in figure 3. For comparison, the correspondent values of table 5 ($E_{f(\text{Table 5})}$) are also shown.

Composites	E_f (GPa)	$E_{f(\text{Table 5})}$ (GPa)	Error (%)
(TbFe+Fe)/Glass	135.9	130.0	4.5
(TbFe+Fe)/Silicon	136.2	130.0	4.7
Aluminium/Sapphire	71.9	70.0	2.7
Tungsten/Aluminium	378.1	400.0	5.5

Figures

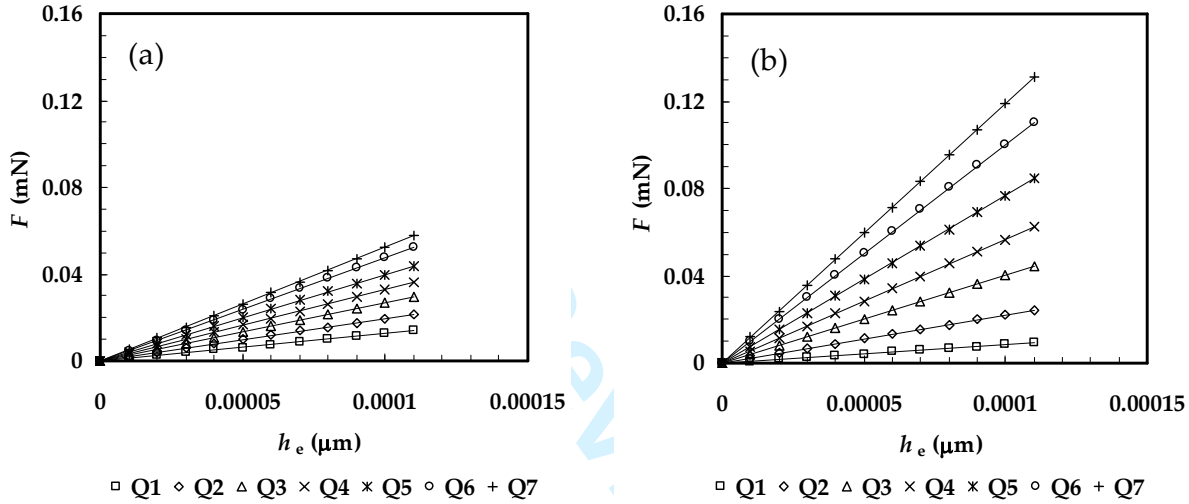

Figure 1. Load *versus* elastic indentation depth, obtained by numerical simulation, using squared flat punch indenters with seven different contact areas: (a) Composite C1 ($E_f / E_s = 4$); (b) Composite C7 ($E_f / E_s = 0.25$).

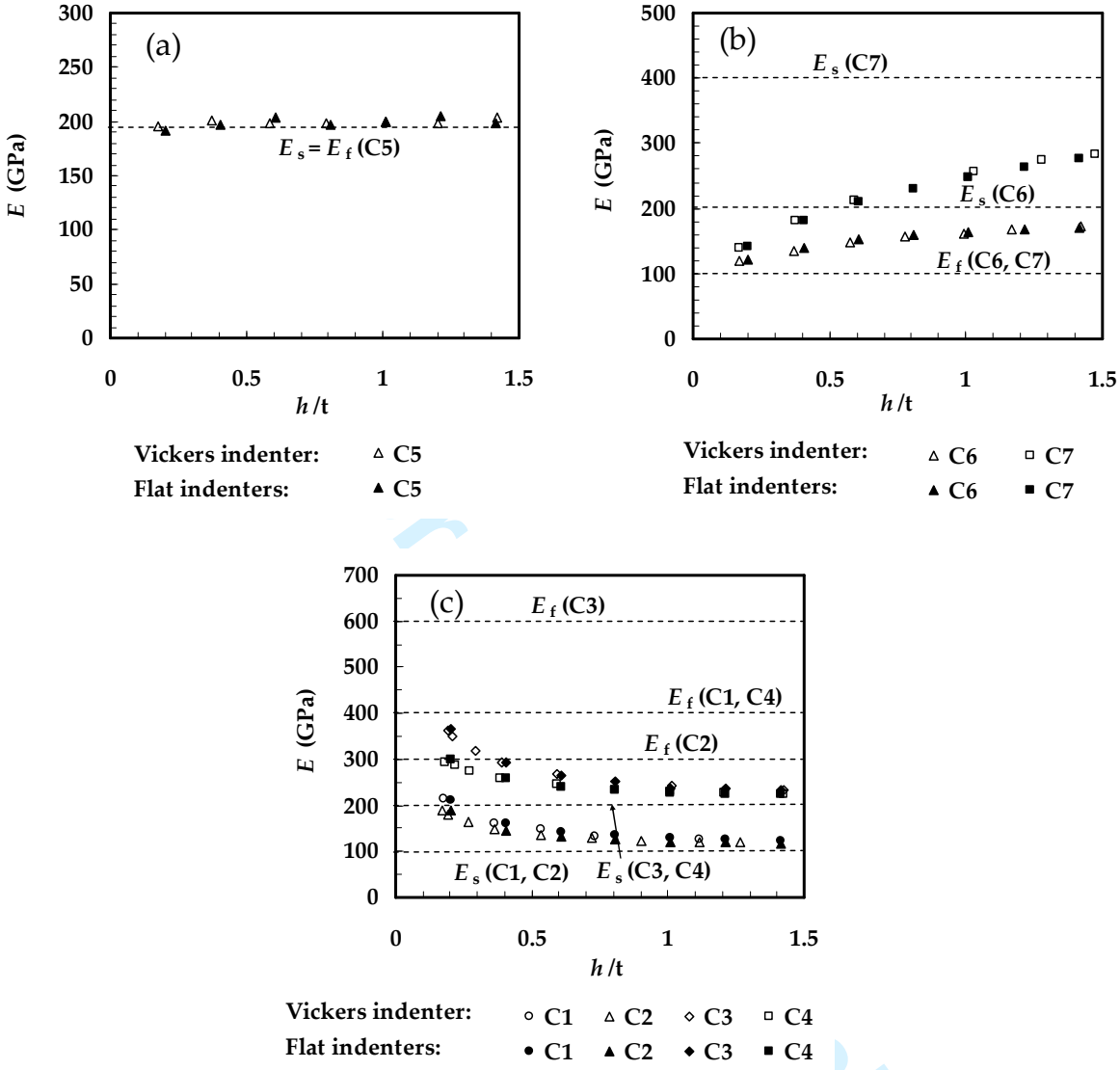

Figure 2. Composite Young's modulus *versus* normalized contact indentation depth, determined with pyramidal and flat punch indenters: (a) $E_f = E_s$; (b) $E_f < E_s$; (c) $E_f > E_s$.

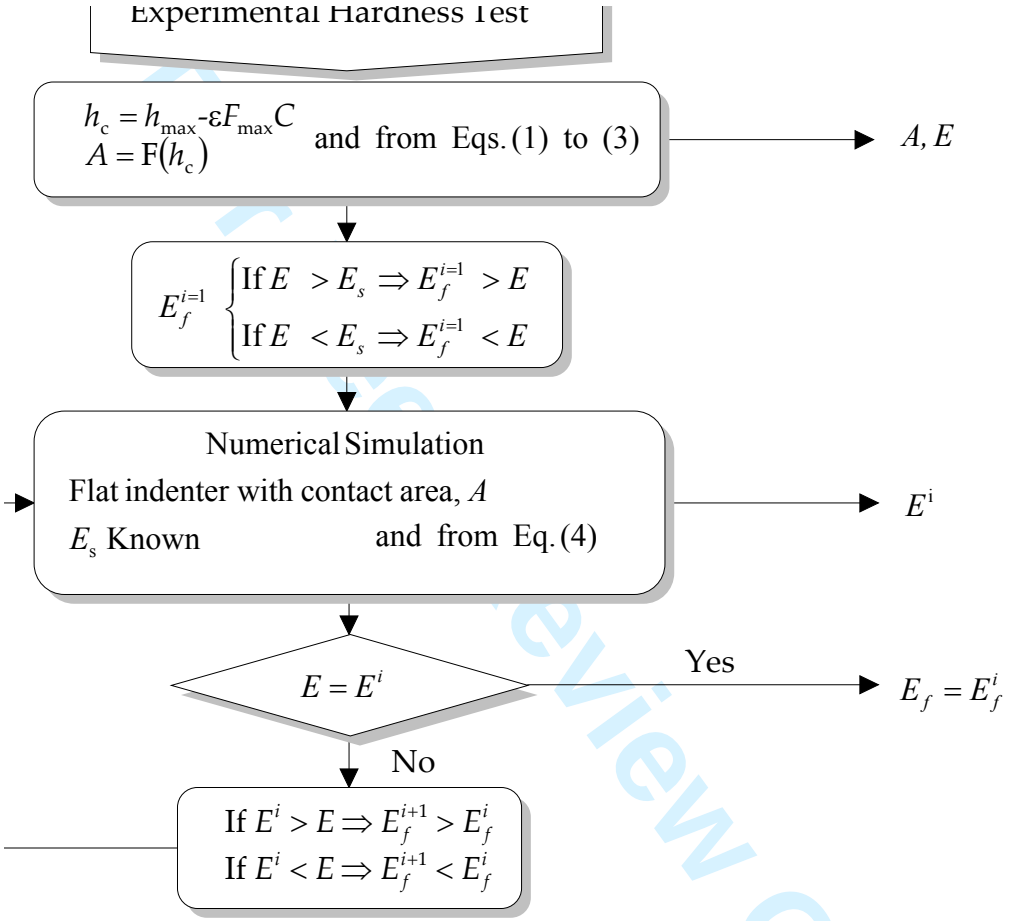

Figure 3. Reverse analyses algorithm for thin film Young's modulus determination.

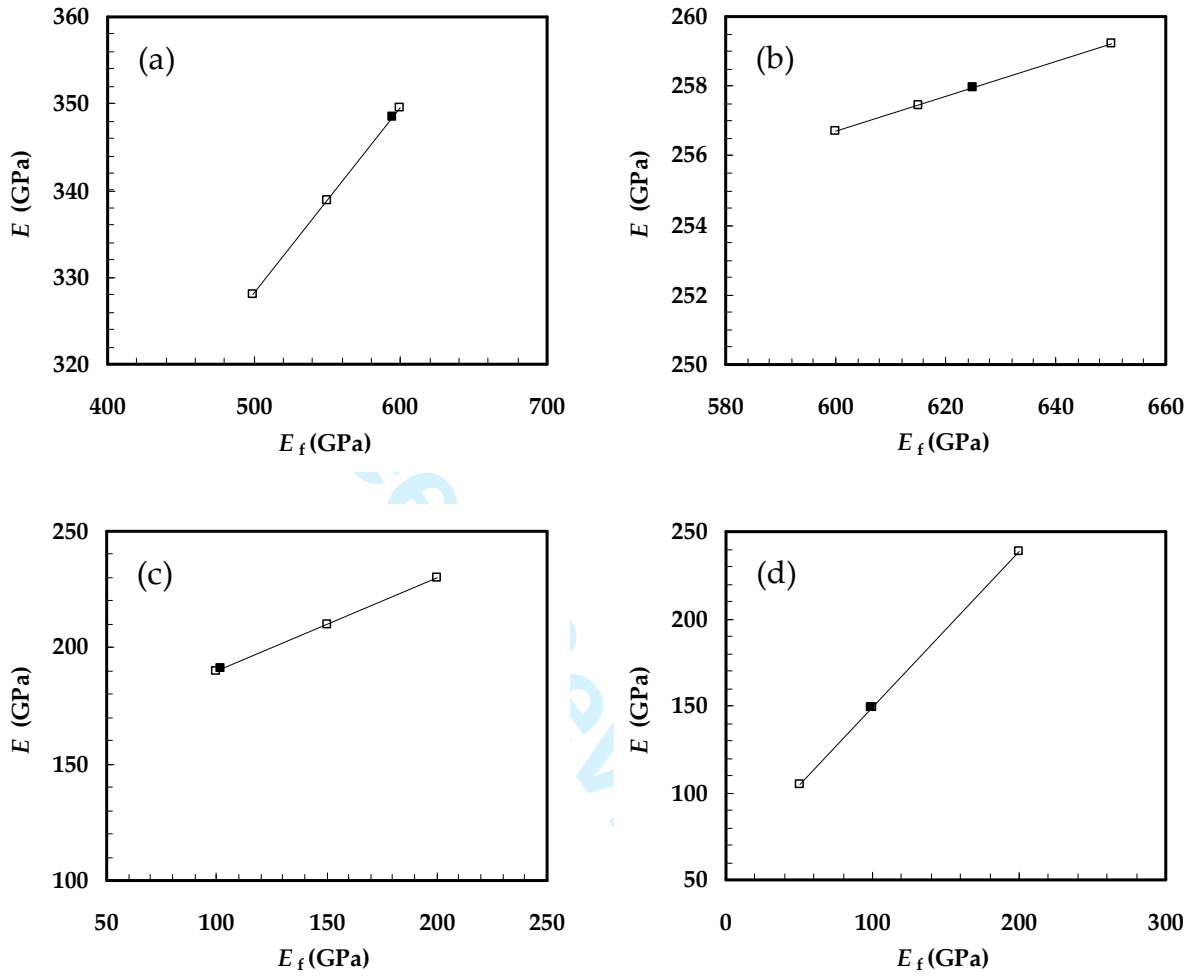

Figure 4. Composite Young's modulus ($E = E^{\mathrm{i}}$) *versus* the film Young's modulus ($E_f = E_f^i$), obtained for the composites C3 and C6, at two different equivalent contact indentation depths: (a) Composite C3 and $h/\mathrm{t} = 0.2$; (b) Composite C3 and $h/\mathrm{t} = 1.3$; (c) Composite C6 and $h/\mathrm{t} = 0.3$; (d) Composite C6 and $h/\mathrm{t} = 1.3$.

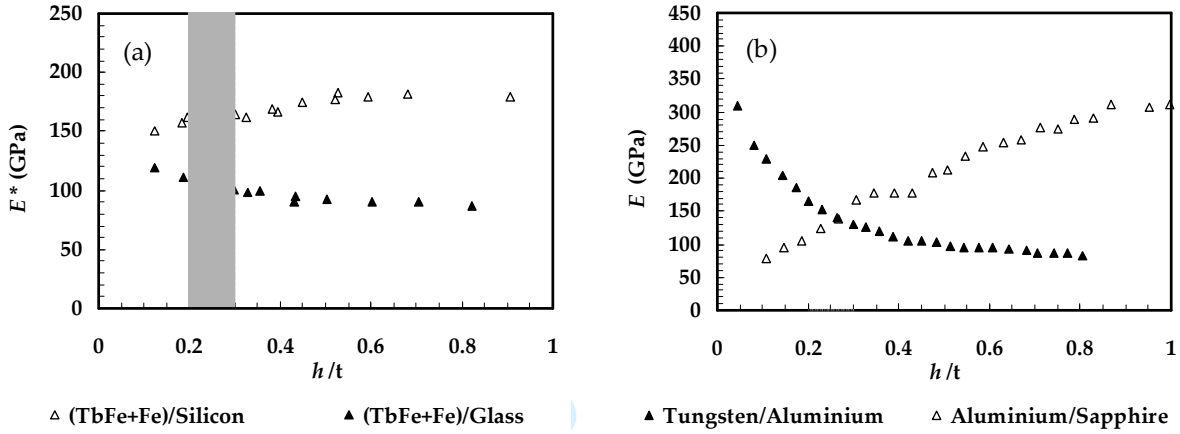

Figure 5. Composite Young's modulus *versus* relative indentation depth. (a) Experimental data by Menčík *et al.* [10]: Composites (TbFe+Fe)/Silicon and (TbFe+Fe)/Glass. (b) Experimental data by Saha and Nix [6]: Composites Tungsten/Aluminium and Aluminium/Sapphire.